

## A New Experimental Approach to Validation of Aerodynamic Derivatives Based Model for Self-Excited Forces

B. Siedziako<sup>1</sup>, O. Øiseth<sup>1</sup>

<sup>1</sup>Department of Structural Engineering, Norwegian University of Science and Technology, Trondheim 7491, Norway

### Abstract

A new methodology to validate Scanlan’s model for self-excited forces for bridge decks is proposed in this paper. The method is based on a new experimental setup capable of forcing a section model in a motion that resembles the actual behavior of the bridge deck in full scale. The reliability of the model involving aerodynamic derivatives identified applying the standard forced vibration procedure is validated by examining whether the model can predict self-excited forces when bridge deck is forced in the motion obtained by solving the equation of motion for the entire bridge. The bridge deck of the Hardanger Bridge is used as a case study considering flutter motion and the bridge response for a mean wind velocity of 50 m/s. The results show the aerodynamic derivatives predict the self-excited lift and pitch with high accuracy, while the self-excited drag force is underestimated.

### Introduction

Aerodynamic derivatives (ADs) are currently one of the most common outputs from wind tunnel tests of bridge decks. They define the relationship between the bridge deck motion and the induced self-excited forces [8] that modify the properties of the combined structure and flow system and may cause certain aeroelastic phenomena, such as flutter or galloping. Reliable estimates of ADs are thus crucial for the design of long-span bridges. The ADs are most commonly identified by section model tests applying either the forced or free vibration technique. The motion of the section model in a free vibration test is considered to be more realistic since it results from mutual interactions between the wind flow and the model, compared to the standard forced vibration technique where the section is forced in a sinusoidal motion. The experimental data from free vibration tests are however more scattered than those obtained from forced vibration tests. A previous study [7] provided insight into the variability of ADs by investigating how different laboratory conditions and testing techniques influence the experimental results. Additionally, variability in the estimated ADs has been addressed in flutter analysis, showing that the resulting critical velocities may differ up to thirty percent [1]. Another study approached flutter using Monte Carlo simulations and modeled uncertainties in the ADs using the expected values, and the covariance matrix of the coefficients obtained by curve-fitting the experimental data [9]. The precise modeling of the geometry and the applied testing method were shown to be important factors for the distribution of the critical flutter speed and obtained confidence bounds. However, it has been shown that ADs might depend on the motion applied during testing [2,4,5]. This raises the question whether ADs identified in a standard procedure can be used to predict the aeroelastic loads induced during motion that resemble actual bridge motion. Therefore, in this study, a new approach to wind tunnel data reliability is proposed. Rather than focusing on the statistical properties of identified coefficients, the authors use experimentally obtained data to predict the self-excited forces induced during realistic bridge motion at two mean wind speeds: 50 m/s and 82.4 m/s (the latter represents the critical flutter speed of the Hardanger Bridge).

### Case Study – Hardanger Bridge

The Hardanger Bridge is currently the longest suspension bridge in Norway. With a 1310 m long main span and only an 18.3 m wide bridge deck, it is an excellent example of a slender structure. Figure 1 presents the cross-section of the bridge deck section model used for wind tunnel testing in this study that corresponds well with the actual bridge geometry [9].

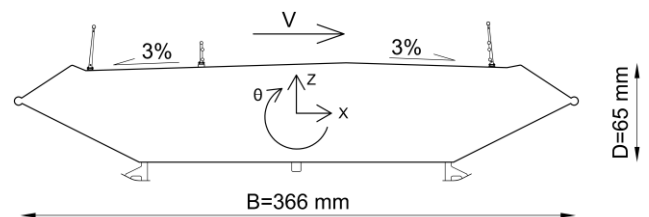


Figure 1. Cross-sectional dimensions of the Hardanger Bridge section model used in this study. Model scale is 1:50.

To simulate in the wind tunnel realistic in-wind behavior of the bridge deck, multi-mode flutter analysis and buffeting analysis using a velocity of  $V=50$  m/s were conducted. Due to page limitations, the authors refer to the following publications [9,14] for details on the calculations since the computational procedures are not the primary focus of this study. It should be noted that the motion of the bridge deck differs along its longitudinal axis. In this study, the motion at the middle of the bridge deck is considered. The ADs of the Hardanger Bridge section model that included railings and guide vanes used in this study can be found in [9]. To avoid testing extremely low frequencies and high amplitudes, the motion was scaled using frequency and geometric scales ( $S_f$  and  $S_g$ ), concurrently fulfilling similarity requirements:

Variable	Velocity	Geometry	Frequency
Scale factor	$S_g \cdot S_f$	$S_g$	$S_f$

Table 1. Coefficients used when scaling actual bridge motion. Geometric and frequency scales of  $S_g=1/50$  and  $S_f=6$ , respectively, were used in this study.

The motion that reflects the in-wind behavior of the bridge deck at the mid-span of the Hardanger Bridge was generated from the spectral density matrix of the response using Monte Carlo simulations [10]. Figure 2 shows the motion spectra, scaled according to Table 1, used for generating the time series.

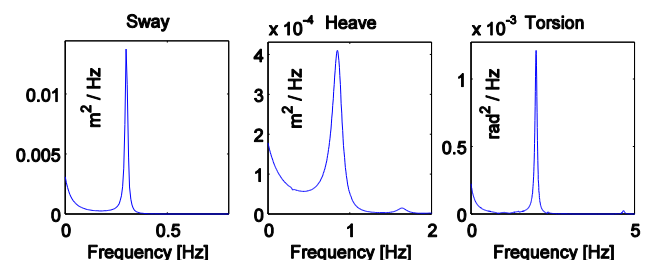


Figure 2. Scaled auto-spectral density matrix of the response of the Hardanger Bridge at  $V=50$  m/s used to generate time series.

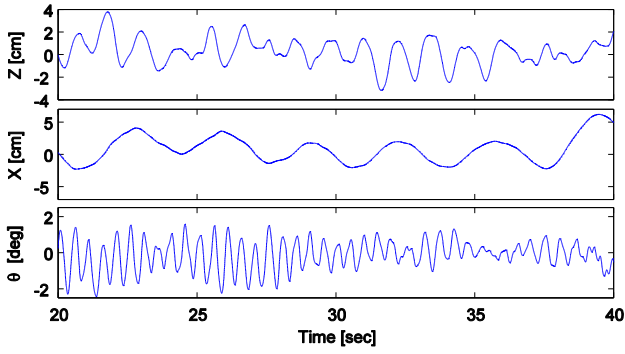


Figure 3. A time series of displacements generated using the scaled spectral density matrix of the response obtained from buffeting analysis.

Multi-mode flutter analysis yields 82.4 m/s and 1.75 rad/s for the critical wind velocity and critical frequency, respectively [9]. To investigate induced self-excited under different vibration amplitudes, flutter motion was obtained by assigning negative damping  $\xi_s = -0.15\%$  to the extracted critical mode shape. Therefore, flutter motion consists of harmonic oscillations and an exponential term that increases the vibration amplitudes with time. Figure 4 shows the pattern of the amplitude growth and the Argand diagram with visible phase angles between the swaying, heaving and pitching harmonic vibrations.

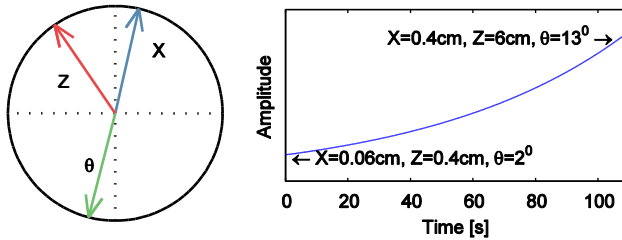


Figure 4. Argand diagram showing flutter mode complexity (left) and the pattern of increasing harmonic oscillations (right) due to the introduction of negative damping. The amplitudes of the motion at the beginning and at the end of the time series are indicated.

The duration of both tests in this study was 110 s.

### Experimental Results

The recently developed experimental forced vibration setup displayed in Figure 4 was used in this study [10]. It was designed specifically to enable measurement of the self-excited forces induced during execution of arbitrary motion. The section model of the bridge deck can be forced into simultaneous swaying, heaving and pitching vibrations, according to an uploaded time series of displacements.



Figure 4. Experimental setup at NTNU [10]. Visualization of the part of the wind tunnel test section with the forced vibration rig.

A control algorithm executed at 20 kHz ensures that the two actuators on either side of the wind tunnel exactly follow the requested motion histories, driving the section model into

motion. Two load cells attached on the both end of the section model measure three force and three moment components during the experiments. Additional information about the components and test conditions can be found in [10] and [11]. In this study, the self-excited forces were obtained using the “Wind-No Wind” method [3,10], in which inertia forces are subtracted from the total forces measured by repeating the tests in still-air.

### Bridge Deck Motion at $V=50$ m/s

The transfer function between bridge motion and self-excited calculated with experimentally obtained ADs can be found only at discrete reduced velocities. Although as Figure 2 shows, the bridge motion is dominated by a single frequency component in each direction, a continuous transfer function is needed for time domain simulations of the aeroelastic forces. Therefore, Rational Function Approximation (RFA) [5] was used in this study to investigate whether ADs extracted in a standard technique can provide reliable predictions of the self-excited forces induced during realistic bridge deck motion. RFA provides a frequency-independent description of self-excited forces using Rational Function Coefficients (RFCs) that define the motion to self-excited force continuous transfer function in the Laplace domain. Representing self-excited forces using RFCs also enables their inclusion in the state-space realization so that time domain simulations may be easily performed [13]. In this study, RFA with two lag terms was used to obtain RFC for all 18 aerodynamic derivatives. Figure 5 compares the experimental data with the RFA result for four ADs considered the most influential.

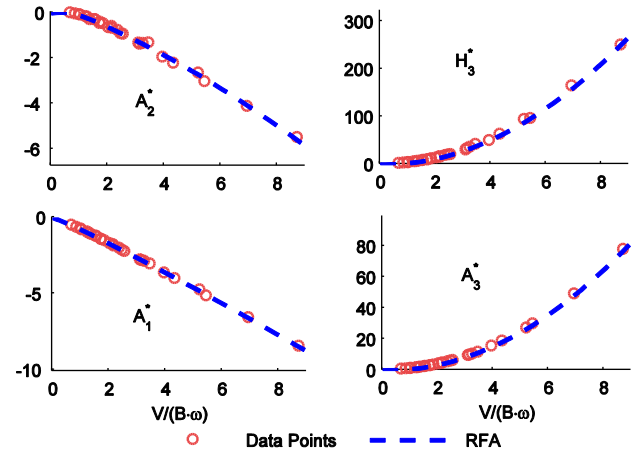


Figure 5. RFA for experimentally obtained aerodynamic derivatives.

According to Table 1, the generated motion was tested at a wind speed of  $V=6$  m/s to satisfy the scaling laws. Figure 6 presents a section of the time series with measured and predicted (using obtained RFCs) values of self-excited forces, while Table 2 shows the correlation coefficient and R-squared ( $R^2$ ) values between measurements and prediction for each of the force components.

Drag		Lift		Pitch	
$\rho_{xy}$	$R^2$	$\rho_{xy}$	$R^2$	$\rho_{xy}$	$R^2$
0.431	0.184	0.947	0.896	0.984	0.967

Table 2. Correlation coefficients and  $R^2$  values between predicted with RFCs and measured self-excited forces.

The experimental results show that the ADs presented in [9], obtained with a standard forced vibration procedure that involves harmonic oscillations, can be successfully used to predict the self-excited pitching moment and lift force when the bridge deck moves in a realistic manner. Almost an excellent match between

the predicted and measured pitch was observed, minor deviations were observed in the case of the lift force, while drag force was seriously underestimated. Although this self-excited component is considered the least significant, the low degree of prediction accuracy is alarming, especially when comparing the  $R^2$  value with those obtained for the lift or pitch. Therefore, the ADs related to drag force identified in standard forced vibration tests are insufficient tools to examine the realistic motion of the Hardanger Bridge.

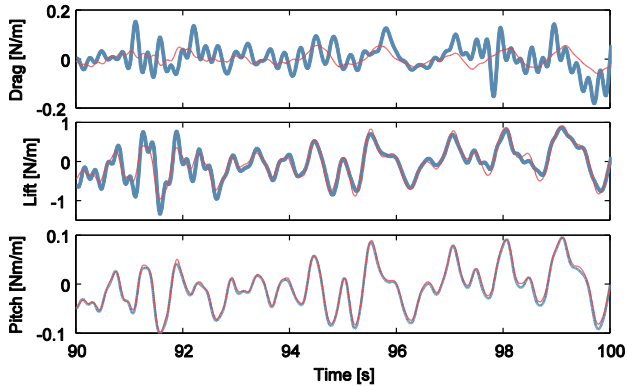


Figure 6. A section of the time series of measured (blue) and predicted (red) self-excited forces induced during simulated mid-span motion of the Hardanger Bridge at  $V=50$  m/s.

This finding demonstrates that the induced self-excited drag force might be sensitive to the applied motion and indicates that the linear load model introduced in [8] may not yield accurate results for this force component.

#### Flutter Motion

The flutter motion studied in this paper research is the sum of harmonic oscillations and an exponential contribution, increasing vibration amplitudes over time to simulate divergent oscillations of the bridge by applying negative damping. Since the damping ratio assigned to the flutter mode is relatively small, the motion considered here is extremely narrow-banded. Therefore, the self-excited forces induced during this type of vibration have been calculated using the expressions given by Scanlan and Tomko [7] derived for sinusoidal motions. The aeroelastic forces, linearly dependent on the bridge deck motion, can then be found knowing the ADs of the Hardanger Bridge at one particular reduced velocity. Since the scaling laws from Table 1 must be fulfilled, the reduced frequency at which flutter occurs ( $V_{red} = 2.57$ ) is the same in the flutter analysis of the Hardanger Bridge and during the wind tunnel testing with the section model. Table 3 compares the critical wind velocities and critical motion frequencies obtained from the multi-mode frequency analysis with the ones used in the wind tunnel calculated based on Table 1 scaling, assuming a frequency scale of  $S_f=6$ .

Critical wind speed		Critical frequency	
Analysis	Wind tunnel	Analysis	Wind tunnel
82.4 m/s	9.89 m/s	0.279 Hz	1.67 Hz

Table 3. Comparison of wind tunnel and on-site conditions during flutter of the Hardanger Bridge.

The 18 aeroelastic coefficients used for force predictions were calculated based on a third-order polynomial fit to the ADs identified during single-DOF harmonic oscillations and are presented in [9]. Figure 7 shows how the  $R^2$  values calculated between the measured and predicted self-excited drag, lift and pitching moment change together with increased flutter motion vibration amplitudes. The results show that for all force components, the  $R^2$  values at the beginning of the time series are

higher than at the end when the vibrations are the largest. However, for the lift and pitch components, changes in the calculated  $R^2$  coefficients are almost negligible since the predicted forces match the measured forces almost perfectly, regardless of the vibration amplitude. However, similar to the case of buffeting response, the  $R^2$  values for the self-excited drag force are much lower than for the lift and pitch. Moreover, a general trend showing a nearly linear decrease from  $R^2=0.6$  to  $R^2=0.2$  is observed for this component, indicating that the prediction accuracy for aeroelastic drag strongly depends on the vibration amplitude.

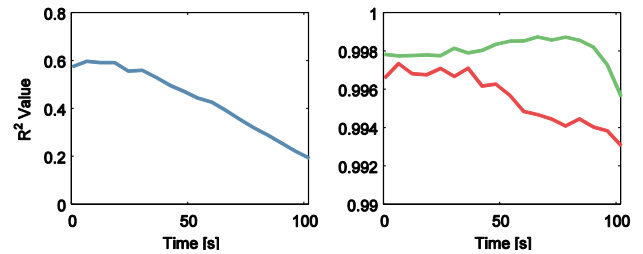


Figure 7. The coefficient of determination calculated between measured and predicted self-excited drag (blue), lift (red) and pitching moment (green).

To further investigate the underlying mechanism of the declining  $R^2$  values, the frequency content of the measured aeroelastic forces was examined. Figure 8 shows spectrograms of the self-excited drag, lift and pitching moment. Spectrogram values were scaled to show the relative amplitude of the harmonic signal and allow identification of the dominant harmonic component in the recorded signal.

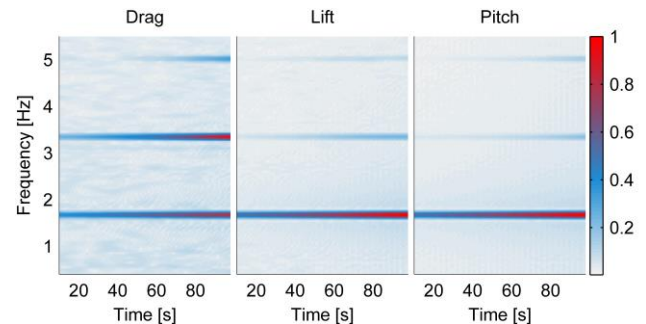


Figure 8. Spectrograms of the aeroelastic forces recorded during simulation of the flutter motion at the mid-span of the Hardanger Bridge. Value 1 indicates the largest recorded amplitude of the single harmonic measured throughout the test duration.

The results presented in Figure 8 explain the decrease of  $R^2$  values between the measured and predicted self-excited forces when the flutter mode strengthens. Although the section model moves utilizing nearly only single motion frequency, which is the critical flutter frequency  $\omega=1.67$  Hz, higher-order harmonic contributions at  $2\omega$  and  $3\omega$  start to appear in the measured forces as the vibration amplitudes increase. For the lift and pitching moment, those effects build up very slowly and the relative magnitude of the higher-order harmonics is small compared with the dominating first-order harmonic. Therefore, the linear load model based on the ADs [8] yields very good results when predicting those aeroelastic forces. However, for the drag force, the first-order harmonic dominates only at the beginning of the experiment, when vibration amplitudes are low. As the amplitudes grow, other harmonic contributions that are not considered in the applied load model start to play an important role. In particular, the second-order harmonic at  $2\omega$  becomes crucial since its magnitude increases much faster than the first-order harmonic. The presence of the higher-order harmonics in the self-excited forces at fixed motion amplitudes has been reported previously by [2] for the lift and pitch components, and

later by [13] for the self-excited drag force based on computational fluid dynamics simulations. Current study emphasizes the significance of the motion amplitude as a primary factor determining the magnitude of the higher-order contributions.

## Conclusions

In this paper, a new methodology to assess the reliability of extracted aerodynamic derivatives is proposed. The goal of the described method is to investigate whether aerodynamic derivatives identified in a standard procedure can predict motion-dependent forces for conditions and motions that resemble those of an actual bridge. Depending on the correlation between the measured and predicted forces, the reliability of the aerodynamic derivatives can be evaluated. In this study,  $R^2$  values were used to assess that correlation. If successful, the proposed approach highly increases the credibility of using the aerodynamic derivatives identified in wind tunnel tests for predicting the bridge response.

In this study, motion at the mid-span of the Hardanger Bridge was reproduced in the wind tunnel for two cases. First, the motion simulating the bridge deck buffeting response at the mean wind velocity of 50 m/s was considered. Next, flutter motion with divergent vibration character was simulated in the wind tunnel. RFA was applied to predict the self-excited forces during the buffeting response, while the Scanlan and Tomko load model was used to calculate the aeroelastic forces induced during flutter. The experimental results showed that the  $A_i^*$  and  $H_i^*$  aerodynamic derivatives that define the self-excited lift force and pitching moment, identified in standard tests with a forced vibration technique, can be considered extremely reliable since the predicted values for those force components correspond almost perfectly to measured ones in both tests. However, the six aerodynamic derivatives ( $P_i^*$ ) that link bridge deck motion with drag force were not able to accurately predict this force component in the tests. The drag force was underestimated and tests under flutter motion revealed significant contributions to this force component from higher-order harmonics. This indicates that the model used in this study to predict aeroelastic force, together with identified aerodynamic derivatives, are insufficient tools to achieve a reliable estimation of the self-excited drag.

## Acknowledgments

This research was conducted with financial support from the Norwegian Public Roads Administration. The authors gratefully acknowledge this support.

## References

- [1] Caracoglia, L., Sarkar, P. P., Haan, F. L., Sato, H., & J. Murakoshi, Comparative and sensitivity study of flutter derivatives of selected bridge deck sections, Part 2: Implications on the aerodynamic stability of long-span bridges, *Eng. Struct.*, 31, 2009, 2194–2202.
- [2] Chen, Z. Q., Yu, X. D., Yang, G. & Spencer, B. F., Wind-Induced Self-Excited Loads on Bridges, *J. Struct. Eng.*, 131, 2005, 1783–93.
- [3] Diana, G., Resta, F., Zasso, A., Belloli, M. & Rocchi, A., Forced motion and free motion aeroelastic tests on a new concept dynamometric section model of the Messina suspension bridge, *J. Wind Eng. Ind. Aerodyn.*, 92, 2004, 441–462.
- [4] Matsumoto, M., Shiraishi, N., Shirato, H., Shigetaka, K. & Niihara, Y., Aerodynamic derivatives of coupled/hybrid flutter of fundamental structural sections, *J. Wind Eng. Ind. Aerodyn.*, 49, 1993, 575–584.
- [5] Qin, X. R., Kwok, K. C. S., Fok, C. H. & Hitchcock, P. A., Effects of frequency ratio on bridge aerodynamics determined by free-decay sectional model tests, *Wind Struct.*, 12, 2009, 413–424.
- [6] Roger, K. L., *Airplane Math Modeling and Active Aeroelastic Control Design[C]*, AGARD-CP-228, 1977.
- [7] Sarkar, P. P., Caracoglia, L., Haan, F. L., Sato, H. & Murakoshi, J., Comparative and sensitivity study of flutter derivatives of selected bridge deck sections, Part 1: Analysis of inter-laboratory experimental data, *Eng. Struct.*, 31, 2009, 158–169.
- [8] Scanlan, R. H. & Tomko, J., Airfoil and bridge deck flutter derivatives, *J. Eng. Mech. Div.*, 97, 1971, 1717–33.
- [9] Siedziako, B. & Øiseth, O., On the importance of cross-sectional details in the wind tunnel testing of bridge deck section models, in *Procedia Eng. X Int. Conf. Struct. Dyn. EUROLYN*, 2017, (in press).
- [10] Siedziako, B., & Øiseth, O. & Rønnquist, A., An enhanced forced vibration rig for wind tunnel testing of bridge deck section models in arbitrary motion, *J. Wind Eng. Ind. Aerodyn.*, 164, 2017, 152–163.
- [11] Siedziako, B., & Øiseth, O. & Rønnquist, A., A new setup for section model tests of bridge decks, in *Proc. 12th UK Conf. Wind Eng.*, 2016.
- [12] Xu, F. Y., Wu, T., Ying, X. Y., & Kareem, A., Higher-order Self-Excited Drag Forces on Bridge Decks, *J. Eng. Mech.*, 142, 2016.
- [13] Øiseth, O., Rønnquist, A. & Sigbjörnsson, R., Simplified prediction of wind-induced response and stability limit of slender long-span suspension bridges, based on modified quasi-steady theory: A case study, *J. Wind Eng. Ind. Aerodyn.*, 98, 2010, 730–741.
- [14] Øiseth, O., Rønnquist, A. & Sigbjörnsson, R., Time domain modeling of self-excited aerodynamic forces for cable-supported bridges: A comparative study, *Comput. Struct.*, 89, 2011, 1306–22.